Indian J. Phys. **64A** (1), 55-62 (1990)

α-n final state interaction in the break-up of deuterons by α-particles of 45 MeV

A De, S S Dasgupta, D Sen, T Roychoudhury, S N Chintalapudi[+], S R Banerjee[+] and A S Divatia[+]
Department of Physics, Burdwan University, Golapbag, Burdwan-713 104, India

Received 10 April 1989, accepted 3 October 1989

Abstract : Alpha-neutron (α-n) final state interaction (FSI) has been investigated in the break-up of deutron by α-particles of 45 MeV. The line shapes predicted by single level *R*-matrix theory is, in general, acceptable. Effective range theory provides no better fit to the data.

Keywords : Alpha-neutron final state interaction, single level *R*-matrix theory, effective range theory.

PACS No : 25.10+s

1. Introduction

Recently considerable attention has been focussed on the study of alpha-deuteron interaction, both theoretically and experimentally, with an emphasis on fitting the data provided by kinematically complete experiments (Gaiser *et al* 1988 and the references therein). Alpha-deuteron system, being a six nucleon assembly, is of particular interest because at low energies (below α-break-up threshold) it could be treated as a simple three body system made up of a structureless α-particle, a proton and a neutron. Final state interactions which may be due to any one, two or all the three pairs (α*p*, α*n* and *pn*) of outgoing particles and which, often play an important role in understanding the break-up reaction mechanism, has been the subject of significant interest by several workers (Bruno *et al* 1980, Sagara *et al* 1977, Warner and Bercaw 1968). Considerable success has been achieved by the authors in fitting the line shapes of FSI peaks in the light of single level *R*-matrix calculations. Calculations based on effective range theory has also been used fruitfully in fitting the break-up data at low energies (Dasgupta *et al* 1980a, b). The present paper is an endevour to carry out analysis of α-*n* interaction at 45 MeV alpha-energy, using both the methods referred above.

[+]Variable Energy Cyclotron Centre, BARC, Calcutta-700 064, India.

2. The experiment

The experiment was carried out at the Variable Energy Cyclotron Centre, Calcutta using α-particles of 45 MeV. Experimental details and some of our experimental data have been reported elsewhere (Dasgupta *et al* 1989). Si(Li) detectors were used to detect α-particles and protons in coincidence. The target used was deuterated polyethylene foil. The energy and correlated pairs of angles were chosen so as to favour highly the α-*n* interaction alone in the allowed phase space. Figure 1 shows

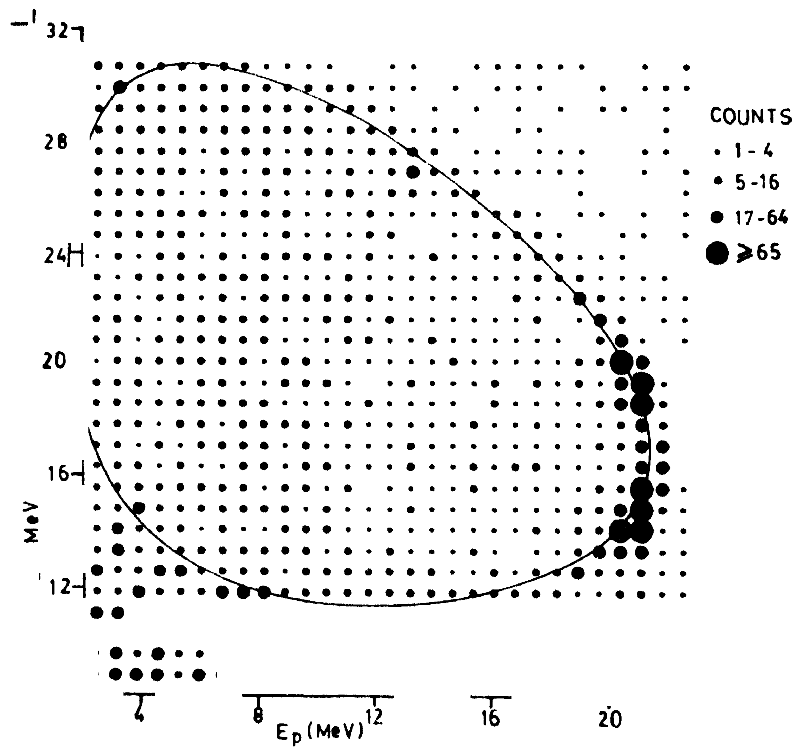

Figure 1. Bi-dimensional representation of the α*p* coincident events at $\theta_\alpha = 20°$, $\theta_p = 40°$ with the nominal kinematic curve superimposed on it, E_α (inc) = 45 MeV.

one of the bidimensional spectra (20°, 40°) with the nominal kinematic curve superimposed on it.

3. Method of analysis

Before applying any specific method to analyse the experimental data, we recall the particular kinematical situations we considered. The allowed phase space for each of the angular combinations favours the regions of ^{5}He-ground state formation ($E_{\alpha n} \simeq 0.9$ MeV) and at the same time, production of ^{5}Li-ground state ($E_{\alpha p} \simeq 1.9$ MeV) and occurrence of *np* FSI ($E_{np} \simeq 0$ MeV) are almost discarded solely from the kinematical point of view. As shown by the relative energy curves in Figure 2, the latter two points are never reached in the angular combinations considered. In the figure, the relative energies $E_{n\alpha}$, $E_{p\alpha}$ and E_{pn} corresponding to the three final particles are shown by the dashed dotted curves marked accordingly. For the two values of E_α where $E_{\alpha n} \simeq 0.9$ MeV, the

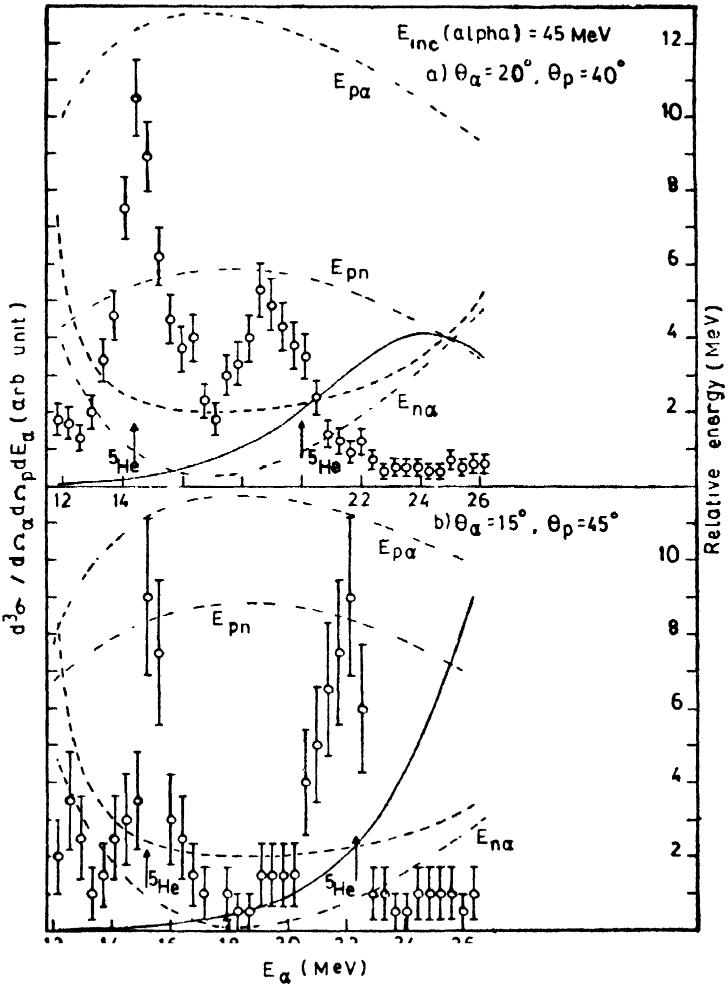

Figure 2. Differential cross section $d^3\sigma/d\Omega_\alpha d\Omega_p dE_\alpha$ (in arbitrary unit) against E_α (MeV) for (a) $\theta_\alpha=20°$, $\theta_p=40°$ and (b) $\theta_\alpha=15°$, $\theta_p=45°$ with $\Phi_\alpha=180°$, $\Phi_p=0°$ and incident energy=45 MeV (alpha). Dashed-dotted curves are the relative energies in MeV (right scale) of the outgoing particles as indicated. Dashed and solid curves are the PWIA calculations (arbitrary unit) corresponding to proton spectator and neutron spectator, respectively. The arrow marks indicate the kinematically predicted ^{5}He–ground state positions.

corresponding other two relative energies are much higher and far away from those needed for ^{5}Li-ground state or np FSI phenomena to manifest. From the curves, it is highly expected that the spectra of the cross sections might be influenced most by the αn FSI leading to ^{5}He-ground state formation.

Now, the three body break-up amplitude in a rigorous theory like that based on Faddeev's three body formalism, must include the αp and αn impulse terms and all the three multiple scattering terms corresponding to the three pairs as mentioned. However, in this paper we have no intention of going into the full theoretical formulations. We are rather guided somewhat empirically to fit the shape of the measured spectra in terms of the standard approximations as used by other workers.

Plane wave impulse approximation (PWIA) (Kuckes *et al* 1961, Warner and Bercaw 1968) is inadequate to reproduce the spectra in the present case as indicated by the dashed and solid curves in Figure 2. None of the PWIA contributions, αn (dashed curve) or αp (solid curve) indicate any enhancement in the positions where sharp peaks are actually observed in the measured spectra. This is due to the very nature of the approximation (PWIA) where the distribution has been mainly governed by the spectator energies.

As the experimentally observed peak positions (Figure 2) undoubtedly correspond to the kinematically predicted regions for ^{5}He-ground state, we were intended to fit the measured spectra assuming αn FSI alone.

We give an outline of the following two methods which we used for FSI analysis.

3.1. *R-matrix calculation :*

In single level *R*-matrix theory following the procedure of Werntz (1962) and as suggested by Sagara *et al* (1977), near strong αn FSI which is assumed to be in $P_{3/2}$ state, the cross section may be written as

$$d^3\sigma/d\Omega_\alpha d\Omega_p dE_\alpha = N \sin^2 \delta_1[F_1^2(ka)+G_1^2(ka)]\rho/(ka)^2 \tag{1}$$

where N is a factor dependent on the incident energy alone, δ_1 is the $P_{3/2}$ resonant phase shift, F_1 and G_1 are the neutron wave functions and $\hbar k$ is the αn relative momentum. The phase shift δ_1 is calculated using the relation

$$\tan \delta_1 = \tfrac{1}{2}\Gamma/(E_0+\Delta_1-E_{\alpha n}) \tag{2}$$

where

$$\Delta_1 = -\tfrac{1}{2}\Gamma/(F_1F_1'+G_1G_1') \tag{3}$$

and

$$\tfrac{1}{2}\Gamma = \gamma^2 ka/(F_1^2+G_1^2). \tag{4}$$

ρ is the phase space factor given by (Ohlsen 1965, Warner and Bercaw 1968)

$$\rho = 8Ep(E_\alpha)^{1/2}/[(E_p)^{1/2}+(E_\alpha)^{1/2}\cos\theta_{\alpha p}-(E_i)^{1/2}\cos\theta_p] \tag{5}$$

where E_i, E_α and E_p are the lab kinetic energies of the incident and scattered α-particles and the proton, respectively, θ_p the proton scattering angle and $\theta_{\alpha p}$, the included angle between the two detected particles. Three parameters E_0, γ^2 and a are as discussed in Section 4.

Here, we mention that we have omitted the angular dependence factor, namely the $\cos^2\chi$ term, in the right hand side of eq. (1) as was also done by Sagara *et al* (1977), represented by eq. (9) in their paper. Actually, it ($\cos^2\chi$) is taken as constant and the choice is somewhat empirical. χ, the scattering angle of the neutron in the *αn* system, is a model dependent quantity characteristice of single process model. In the presence of dominant multiple processes, at the lower energy like 8.9 MeV E_a ($E_\alpha=17.8$ MeV), this choice ($\cos^2\chi$=constant) has been shown to yield highly satisfactory result. Even at comparatively higher incident energy like 42 MeV (alpha), the same formalism has been seen to work better (Figure 3) than that including the χ-dependence. In Figure 3,

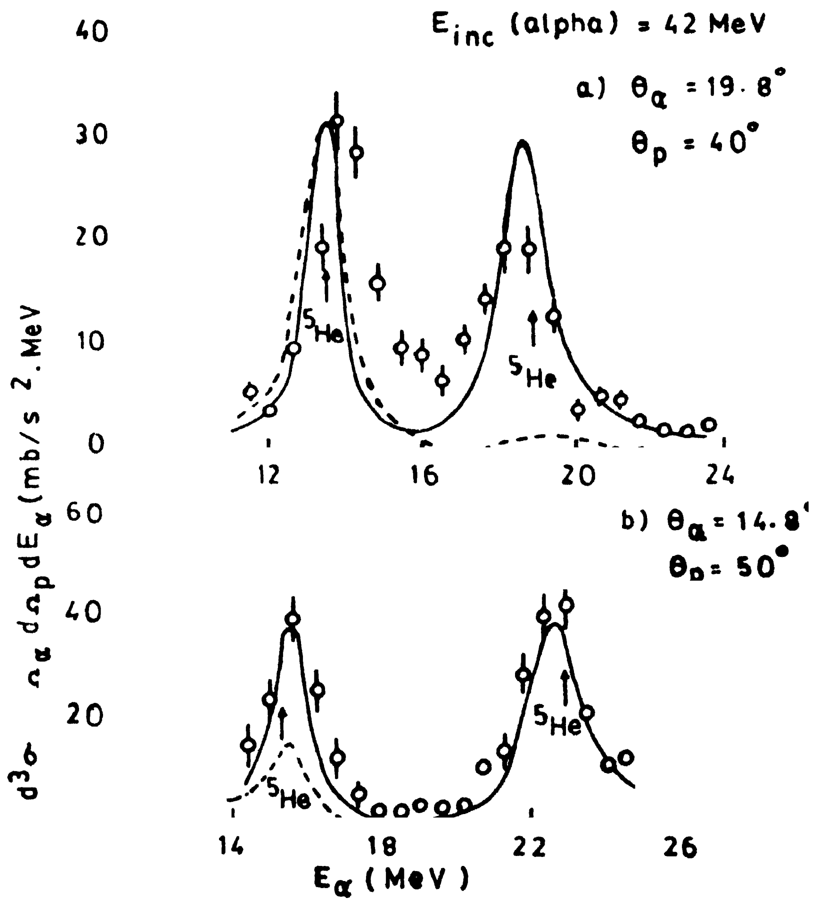

Figure 3. Differential cross section $d^3\sigma/d\Omega_\alpha d\Omega_p dE_\alpha$ (in mb/sr^2. MeV) against E_α (MeV) for (a) $\theta_\alpha=19.8°$, $\theta_p=40°$ and (b) $\theta_\alpha=14.8°$ $\theta_p=50°$ with incident energy of 42 MeV (alpha). The experimental points are from Warner and Bercaw. As stated in the text, the dashed curves result from R-matrix calculations when $\cos^2\chi$ dependence is included while the solid curves are due to the same calculation but with $\cos^2\chi$=Constant.

the dashed curves represent the calculations of Warner and Bercaw (1968) including the $\cos^2 \chi$ factor while the solid curves display the present calculation using eq. (1). For the angular combination $\theta_\alpha = 14.8°$ and $\theta_p = 50°$, both the calculations just coincide at the higher E_α peak, so far as the shape is concerned. For both the angular combinations $(\theta_\alpha, \theta_p) = (19.8°, 40°)$ and $(14.8°, 50°)$, the situation is largely improved when eq. (1) is used and this motivate us to proceed in the same way for the present case at 45 MeV also.

3.2. *Effective range theory :*

Following Watson's relation (Watson 1952) for the effective range approximation in final state interaction theory, we have for αn FSI, the expression representing the squared matrix element as

$$\frac{\sin^2 \delta_l}{k^2} \tag{6}$$

where the phase shift δ_l is given by the relation

$$k^{2l+1} \cot \delta_l = -\frac{1}{a} + \frac{1}{2} rk^2, \tag{7}$$

a and r being the effective range parameters.

4. Results and discussions

As has been already shown in Figure 2, the Figure 4 (a and b) displays the three body differential cross section $d^3\sigma/d\Omega_\alpha d\Omega_p dE_\alpha$ (in arbitrary unit) against E_α (in MeV), for two correlated pairs of angles $(\theta_\alpha, \theta_p) = (20°, 40°)$ (Figure 4a) and $(15°, 45°)$ (Figure 4b). The arrows indicate the position of FSI peaks corresponding to ^{5}He-ground state (Figures a and b) and αp QFS peak (Figure b), solely determined by the kinematical considerations. The QFS peak is at $E_n = 0.19$ MeV, the lowest allowed neutron kinetic energy. The solid curves are the results of R-matrix calculations using the parameters from Dodder and Gammel (1952) which are

$$E_0 = -4.3 \text{ MeV}, \ \gamma^2 = 6.9 \text{ MeV and } a = 2.9 \text{ fm}.$$

So far as the FSI peaks at lower E_α are concerned, the theory predicts the line shapes fairly well, for both the angle pairs. However, the calculated peaks at higher E_α show a small displacement in energy as was also seen by Warner and Bercaw (1968). A slight change of E_0 from -4.3 to -4.6 results in some improvement in these peak positions but the peak cross section degrades the situation (dashed curves), mainly for $(20°, 40°)$ combination. Calculations with little change in other input parameters were performed but no significant improvement was achieved. The dotted curves are the prediction due to effective range

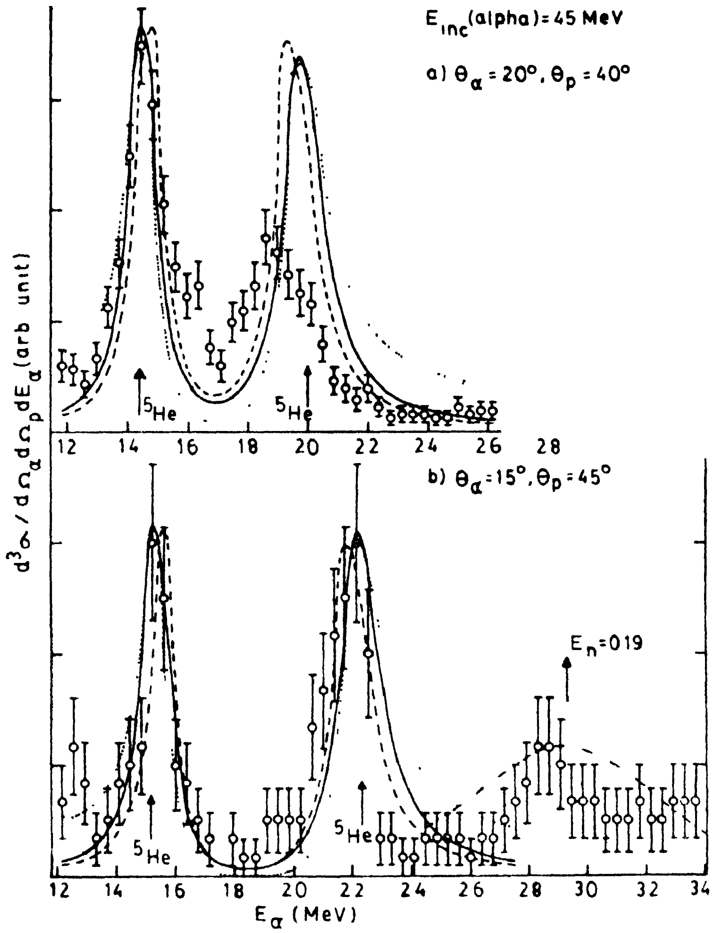

Figure 4. Differential cross section $d^3\sigma/d\Omega_\alpha d\Omega_p dE_\alpha$ (in arbitrary unit) against E_α (MeV) for (a) $\theta_\alpha = 20°$, $\theta_p = 40°$ and (b) $\theta_\alpha = 15°$, $\theta_p = 45°$ with $\Phi_\alpha = 180°$, $\Phi_p = 0°$ and incident energy = 45 MeV (alpha). Solid curves are the results of R-matrix calculation with $\gamma^2 = 6.9$ MeV, $a = 2.9$ fm and $E_0 = -4.3$ MeV. Dashed curves depict the same calculations but with $E_0 = -4.6$ MeV. Dotted curves are the prediction due to effective range theory. The dashed-dotted curve indicates the impulse approximation calculation.

theory using the parameters from Arndt *et al* (1973). As is discerned from the figure at higher E_α, contrary to lower ones, results of effective range theoretical calculations become worse in comparison to that of R-matrix theory. Calculations including $S_{1/2}$ and $P_{1/2}$ states were also peformed (not shown in the figure) using the effective range theory but no improvement was obtained. This, along with R-matrix calculation indicates that the reaction mechanism is mainly governed by the αn FSI in the $P_{3/2}$ state. Analysis using the more sophisticated theory based on Faddeev formalism would be welcome to understand the observed discrepancy in the present analyses.

Though our data has rather poor statistics, we tried to fit the broad peak due to αp QFS in the light of impulse approximation formalism of Burress, as outlined in the paper of Warner and Bercaw. It is indicated by the dashed-dotted curve in Figure 4b. Measurements involving a large amount of data with better statistics is needed to make a systematic study of the problem.

Acknowledgement

Financial support in the form of Research Fellowship from the University of Burdwan is gratefully acknowledged.

References

Arndt R A, Long D D and Roper L D 1973 *Nucl. Phys.* **A209** 429

Bruno M, Cannata F, D'Agostino M, Vannini G, Bongiovanni F, Frisoni M and Lombardi M 1980 *Nuovo Cim. Lett.* **29** 1

Dasgupta S S, Roy R, Rioux C, Lahlou F and Slobodrian R J 1980a *Phys. Lett.* **91B** 32

Dasgupta S S, Slobodrian R J, Roy R, Rioux C and Lahlou F 1980b *Phys. Rev.* **C22** 1815

Dasgupta S S, De A, Sen D, Roychoudhury T, Chintalapudi S N, Banerjee S R and Divatia A S 1989 *Proc. of Few Body XII, Vancouver 1989* (to be published)

Dodder D C and Gammel J L 1952 *Phys. Rev.* **88** 520

Gaiser N O, Darden S E, Luhn R C, Schieck H Paetz gen and Sen S 1988 *Phys. Rev.* **C38** 1119

Kuckes A F, Wilson R and Cooper P F, Jr. 1961 *Ann. of Phys.* **15** 193

Ohlsen G G 1965 *Nucl. Instr. Meth.* **37** 240

Sagara K, Hara M, Takahashi N, Motobayashi T, Takeutchi F, Soga F and Nogami Y 1977 *J. Phys. Soc. Japan* **42** 732

Warner R E and Bercaw R W 1968 *Nucl. Phys.* **A109** 205

Watson K M 1952 *Phys. Rev.* **88** 1163

Werntz C 1962 *Phys. Rev.* **128** 1336